Towards a Real-time Seizure Detection Algorithm for Closed-loop Optogenetic Modulation of an Animal Model of Epilepsy

A Thesis
Presented to
The Academic Faculty

by

Bahar Rahsepar

In Partial Fulfillment
of the Requirements for the Degree
Bachelors of Science in Biomedical Engineering with Research Option in the
School of Biomedical Engineering

Georgia Institute of Technology
December 2014

Towards a Real-time Seizure Detection Algorithm for Closed-loop Optogenetic Modulation of an Animal Model of Epilepsy

Approved by:

Dr. Robert E. Gross
School of Medicine
Emory University
Wallace H. Coulter Dept. of Biomedical Engineering
Georgia Institute of Technology

Dr. Robert J. Butera
School of Electrical and Computer Engineering
Georgia Institute of Technology
Wallace H. Coulter Dept. of Biomedical Engineering
Georgia Institute of Technology

Date Approved: December 12, 2014

ACKNOWLEDGEMENTS

I would like to use this opportunity to express my gratitude to everyone who supported me throughout the course of this biomedical engineering project. I would never been able to finish this project without the guidance of my mentor Dr. Nealen Laxpati, committee members Drs. Robert Gross and Robert Butera, and support from computational neuroscience training program (CNTP). Further I would like to thank my previous research mentors who taught me how to do research and gave me invaluable insights about neuroscience during my rotations in their labs, Drs. Donald Rainnie and Astrid Prinz. Last but not least my supporting family and friends for their unlimited guidance, support and patience with me.

TABLE OF CONTENTS

LIST OF TABLES

LIST OF FIGURES

LIST OF SYMBOLS AND ABBREVIATIONS

PD	Parkinson's Disease
AD	Alzheimer's Dementia
OCD	Obsessive Compulsive Disorder
DBS	Deep Brain Stimulation
RNS	Responsive Neuralstimulation
ILAE	International League Against Epilepsy
FFT	Fast Fourier Transform
WVD	Wigner-Ville Distribution
RI	Reduced Interference
ANN	Artificial Neural Network
SVM	Support Vector Machine
LFP	Local Field Potential
NR	NeuroRighter
MPSD	Mean Power Spectral Density in 12-25 Hz frequency band
MCC	Maximum Cross Correlation
LLN	Line-Length

SUMMARY

Epilepsy is a highly prevalent disease affecting 50 million people worldwide, and 3 million domestically in United States of America. About one-third of the epileptic population does not respond to pharmacological treatment and are classified as medically refractory. Surgical intervention is the alternative solution for this population, however it is not effective in the whole population and leaves 10-15% of the patients deprived of relief from seizures. Deep Brain Stimulation is a novel treatment that is being investigated for this disease. In order to fully understand this treatment, one needs to be informed about the neural circuitry and downstream effects of the stimulation. A powerful investigation needs to be done in closed-loop fashion to tie the stimulation with onset of the seizure, without otherwise affecting the brain. This study evaluates the proper metrics for a real-time algorithm with high detection sensitivity and low latency for a closed-loop setup to be used in the experimental setups of epilepsy research. The study first investigates the previous features used for seizure detection, and implements Line-Length (LLN), Mean Power Spectral Density (MPSD) in 12-25 Hz and Maximum Cross Correlation in its algorithm. Offline performance evaluation of candidates identified LLN and MPSD as powerful features with high sensitivity and low detection latency, which could be implemented in future online algorithms for closed-loop experimental setup.

CHAPTER 1

INTRODUCTION

Epilepsy affects approximately 3 million people in the United States, and 50 million worldwide [1]. About one-third of patients do not respond to current drug treatments and are categorized as medically refractory [2]. Surgical intervention is another approach for this group of patients, however only about 60% respond to this treatment, leaving 10 to 15% of total patients deprived of proper treatment [2]. There is thus a need to develop effective therapies to control epileptic seizures in patients.

Brain stimulation is one emerging technology used in the treatment of various neurological and psychiatric disorders, such as Parkinson's Disease (PD), Alzheimer Dementia (AD), Obsessive Compulsive Disorder (OCD), depression, as well as epilepsy [3]. Each of these diseases requires unique targeting and stimulation patterns, which can be investigated for effectiveness through various animal models as well as clinical trials.

With regards to epilepsy, promising experiments suggest that inducing theta oscillations in the hippocampus can reduce epileptic seizures [4], but the mechanism and circuitry involved is unclear. In fact, despite advancements in the field of epilepsy, the cellular mechanisms underlying the disease itself are also equivocal. Consequently, a mechanistic investigation of the relevant circuitry would provide insight on the disease and advance the therapies available.

Seizures are accompanied by electrographic changes in the electrical recordings from the brain. Both open-loop (e.g. Deep Brain Stimulation (DBS)), and closed-loop (e.g. Responsive Neural Stimulation (RNS)) electrical stimulation devices have been implanted in

clinical cases for the treatment of epilepsy. Their results suggest that the closed-loop systems did not negatively impact cognitive function, whereas during continuous open-loop stimulation in the anterior thalamic nucleus resulted in more subjective depression and memory impairments compared to controls [5]. It is clear that an ideal intervention is capable of interrupting the seizure without otherwise affecting the patient.

In order to best determine targets for neuromodulation and reduce the occurrence of side effects from stimulation, we are investigating optogenetic activation of specific neuron-types in the medial septum for modulation of hippocampal epileptiform activity in the rat tetanus toxin model of epilepsy. Optogenetics is a novel neuromodulatory tool in the field of the neuroscience that enables neuron-type specificity as well as millisecond temporal precision, and has been widely applied in the study of various brain diseases [6]. In order to temporally bind optical intervention with the onset of a seizure, a closed-loop system design is required. A functional closed-loop setup needs an effective real-time seizure detection algorithm that is closely tuned with the experimental model, hardware, and desired outputs stimulation accordingly.

This project is aiming at characterizing seizure events in the tetanus toxin model of epilepsy in rats and developing offline algorithms that are capable of capturing seizure events. Furthermore, by evaluating the offline performance of the algorithms, the ultimate goals of this project are to develop an optimal real-time seizure detection algorithm and implement it in C♯ as a part of the NeuroRighter electrophysiology platform [7] in order to produce an *in viv*o closed-loop optogenetic set-up. This algorithm needs to be capable of identifying a seizure within an effective time window that would allow timely delivery of seizure-arresting stimulation. The goal is to design an algorithm that will be robust and

applicable to different models of epilepsy, such as the tetanus toxin and kainic acid models of temporal lobe epilepsy. Adoption of this system would add temporal specificity of the optogenetics intervention to the onset of the seizure, and will be of use in future optogenetic experiments for epilepsy therapy.

There is extensive literature focused on problem of seizure detection. This thesis will start with a discussion and evaluation of the established methods used for seizure detection, and then to the specific circumstance of Gross Lab experimental setup. It will introduce the methods of the study and further characterize the epileptic data recorded from the rat tetanus toxin model of epilepsy. The investigation continues with choosing metrics for offline analysis and evaluation of performance of these metrics. At the end this thesis I discuss costs and benefits of each of these measures and provide suggestions for future direction in order to get an effective online algorithm for closed-loop optogenetics.

CHAPTER 2

IMPLEMENTED METHODS OF SEIZURE DETECTION

According to International League Against Epilepsy (ILAE), epilepsy is a brain disorder characterized by susceptibility to epileptic seizures and occurrence of at least one epileptic seizure [8]. While there is disagreement over the definition of an epileptic seizure, it is generally defined as abnormal excessive synchronous activity of neurons [8]. This pathologic activity can be observed and quantified in a number of ways, particularly in heterogeneous patients, animal models, and observational methods. More precise definitions are thus subject to more objective requirements based on the general principle of abnormal synchronous activity.

Seizures can be detected in a variety of ways, such as behavioral monitoring, electrocardiogram monitors, and electrographic identification [8]. In the context of this work, seizure detection will consist of an algorithm that identifies the occurrence of ictal events. Offline detection is often sufficient for post-event analysis and quantification purposes. However for the real-time intervention applications, online detection will be required, and it will be necessary to perform this detection as fast, efficiently and precisely as possible. Online analysis and real-time detection of the signal would affect the quality of life of the patients; as it will increase understanding of the disease and make warning systems and closed-loop therapies possible [9]. Online analysis often consists of either seizure detection or seizure prediction, or a combination of the two. Seizure detection identifies a seizure event after its electrographic onset, whereas seizure prediction predicts the occurrence of a future seizure event before its onset [10]. Due to the computational power required for prediction

methods, they are not currently practical for use in an implantable system [11], although there is extensive research on making them computationally efficient.

Work done by Krook-Magnusun et al. [12] is an example of a closed-loop optogenetics system used for study of an effective intervention to stop seizures in an animal model of temporal lobe epilepsy. In their intervention they used kainic acid model of epilepsy in the mouse, and showed that effective optogenetics targeting of neuronal population is capable of stopping seizures. The Neuropace Inc. RNS closed-loop brain stimulation device [13] is an example of clinical closed-loop system for human epilepsy, which showed in a two-year clinical study a statistically significant decrease in the frequency of the seizures. This closed loop system – in contrast to open-loop stimulation systems – benefits from increased battery life, temporally localized and limited stimulation, and decreased side effects associated with long-term continuous stimulation [14].

As a result of the highly non-stationary nature of epileptic seizures, and inter- and intra- individual variability in signal characteristics, automated detection of seizures is difficult and requires a robust and adaptable algorithm [15]. Another obstacle in seizure detection are the inter-ictal activities similar to the seizure onset but which do not fully manifest as seizures [16]. Furthermore, there is no unified definition of the seizures, which makes seizure detection algorithms variable and dependent upon the specific experimental setup and objectives of the study [16]. As a result it is necessary to identify features that make the seizure signals distinct from the other modes of brain activity, as well as signal artifacts, and that apply to our specific experimental paradigm.

Seizure Features

Several studies suggest different identifiable features of seizures in the time-domain, frequency-domain, time-frequency analysis, energy distribution in the time-frequency plane, wavelet features, and chaotic features such as entropy [17]. The following sections provide a brief overview of the analyses that can be performed in order to extract distinct features of the seizure signal and distinguish it from interictal periods. These features can be extracted from various recorded brain signals such as electroencephalography (EEG), electricography (EcoG), as well as the local field potential (LFP), the latter of which will be used in our investigation.

1. Time-domain analysis

Time domain analysis examines a variable in the signal during the time course over which it has been recorded. In time-domain analysis features such as signal amplitude, regularity, synchronicity, and line-length are shown to be effective measure of signal change [17].

1.1. Amplitude

Amplitude is a measure of the instantaneous power of the signal and is historically one of the first measures used in seizure detection [18]. The only problem with this method when employed alone is the high false positive rate due to the noise present in the signal. But this measure serves as an effective feature when used in combination with other measures [19-21]. Generally the amplitude during a seizure signals is higher in comparison to non-seizure activity. This metric is quantified by various means, such as normalized average

amplitude [21], standard deviation from mean [19] and Hajorth parameters [22].

1.1.1. Hajorth parameters

Hajorth parameters are widely used in seizure detection as a measure for quantifying the rate of amplitude changes in the signal, and are defined as activity, mobility and complexity [22]. Since the seizure signal shows faster rate of change, these metrics are shown to be effective measures to distinguish seizure events.

Activity refers to the standard deviation of the signal (σ_s). Mobility is defined as the activity of the first derivative of the signal over the activity of the original signal:

$$\text{Mobility} = \frac{\sigma_{s'}}{\sigma_s}$$

Complexity is the ratio of the first derivative activity over the original signal activity:

$$\text{Complexity} = \frac{\sigma_{s''}/\sigma_{s'}}{\sigma_{s'}/\sigma_s}$$

1.2. Autocorrelation

Autocorrelation analysis is comparison of the signal with itself over a certain time lag, and provides insight over the periodicity of the signal [19]. The electrographic seizure signal is less random and would consequently demonstrate higher autocorrelation values over certain time lag; the proper choice of time lag depends on specific recorded signal.

1.3. Synchronicity

Synchronicity indicates similarity of the two signals, or binding of occurrences of two events [17]. Seizures are primarily characterized by synchronous burst of neurons, besides this activity would spread to further areas and cause the similar synchronous oscillations in the proceeding structures, as a result synchronicity serve as a good indicator of seizure activity.

1.3.1. Phase synchronization and mean phase coherence

Phase synchronization is a measure of how the phases of two oscillators are locked to each other. This concept is applied to the non-linear biological time series and is quantified by the mean phase coherence (R) [23]. This quantity for two time series S_a and S_b is defined as:

$$R = \left|\frac{1}{N} \sum_{j=0}^{N-1} e^{i\,[\Phi a\,(j\,\Delta t) - \Phi b\,(j\,\Delta t)\,]}\right| = 1 - V_C$$

For the discrete time series of length N, $1/\Delta t$ is the sampling rate and V_C is the circular variance calculated from transformation of phase difference to the complex plane unit circle.

1.3.2. Lag synchronization and maximum linear cross correlation

Lag synchronization indicates the similarity of two signals, depending on the acquired signal; this metric can be used to characterize how well two activities are related to each other [23]. As an example, when there are signals from different nearby brain regions, the lag synchronization could be used to determine how the activity of these two regions is related.

One common way to calculate lag synchronization is by cross correlation.

$$S_a (t + \tau) = S_b (t)$$

$$\text{Corr } (S_a, S_b) (\tau) = \int_{-\infty}^{\infty} S_a (t + \tau)\, S_b (t)\, dt$$

As [23] suggests, maximum cross correlation could be serve as actual measure of degree of lag synchronization.

$$\text{Corr}_{max} = \max_{\tau}[Corr\ (Sa, Sb)(\tau)]$$

1.4. Line-length

Line-length is a computationally efficient feature of the LFP time-series that is used for seizure detection. Previous analysis has shown that seizure events are accompanied by increase in rate of change distance between consecutive points of the recorded signal and consequently in value of normalized line-length [24]. Line-length is defined as the distance between the successive points and captures the rate of change in the signal. For seizure detection in sliding window analysis of the signal, normalized line-length is defined as below:

$$\text{LL (n)} = \frac{1}{K} \sum_{k=n-N}^{n} abs\ [\ x(k-1) - x(k)\ ]$$

LL (n) is the normalized line-length that is average value of the distance between successive points inside the sliding window of size N.

2. Frequency-domain analysis

In frequency domain analysis power spectral density (PSD) of the signal is calculated to illustrate the distribution of power in various frequency bands. Various features derived from the PSD can be used for the detection analysis, such as average band frequency, maximum power and dominant frequency [17]. Visual inspection of the PSD from a rat tetanus toxin model of epilepsy shows that in case of the seizure events, power of the signal in 20-40 Hz frequency band is increased.

3. Time-frequency plane

Time-frequency analysis combines frequency domain and time domain analysis resulting in both temporal and frequency specificity that is important in case of the seizures, since they happen at specific time and possess distinct properties in specific frequency bands.

3.1. Spectrographic analysis

Spectrographic analysis decomposes the signal into its power in each frequency band and shows how it varies with time. This analysis is performed via various methods such as Fast Fourier transform (FFT) and short window Fourier transform, Wigner-Ville distribution (WVD), and Reduced Interference (RI) [25].

3.2. Wavelet decomposition

In comparison to the spectrographic analysis using Fast Fourier transform, or the short-time Fourier transform that exhibit a trade off between time and frequency resolution, wavelet decomposition provides a higher resolution analytical alternative [26]. In wavelet

decomposition the signal is approximated in different frequency bands. Debauchies functions are most widely used for seizure detection [17].

4. Chaotic features

Brain activity signals are considered to be chaotic; as a result non-linear dynamics could be applied for effective quantitative analysis of these signals [17]. One of the most widely used chaotic analyses in the seizure detection literature is entropy.

4.1. Entropy

Entropy is a measure of order and disorder in the system, and this concept is developed in information theory, defining the concentration of data in a probability distribution. Since the seizure signal, compared to the normal brain activity is more synchronous and less random, it will show lower entropy values and be distinguishable.

Entropy estimators are categorized into two groups, spectral entropies and embedded entropies. Spectral entropies use the amplitude component of power spectrum while the embedded entropies use the time series directly. Performance analysis of different entropy estimators as presented in Kannathal et al. 2005 shows that although all of the entropy estimator methods yield satisfactory results (above 90% accuracy), Kalmogorov - Sinai entropy, which is representation of the predictability of the signal, demonstrates better performance [27].

Implemented detection algorithms

Historically automatic detection of seizures from EEG recordings started in 1970s

using EEG amplitude, large-amplitude spikes, and spectral analysis [18]. Computational improvements led to the development and implementation of more advanced methods. In general, approaches for seizure detection can be classified in two different categories: threshold based and classifier methods. Examples and practical implementations of both approaches are discussed below.

1. Threshold

In threshold analysis, a segmented signal is analyzed in consecutive windows and compared to either an adaptable or pre-defined threshold. Several studies used threshold based methods for their detection algorithm; summary of some of these approaches can be found in Orosco et al.[17]. An important consideration in using the threshold-based detection is finding the features that are significantly different in seizure versus non-seizure intervals, as well as defining an effective threshold value. Usually these methods are not as highly adaptable or accurate as classifier methods, and they may not serve as an effective approach when high accuracy is a crucial feature for the system.

2. Machine-learning classifiers

Machine learning algorithms are widely used for both seizure detection and prediction. Machine-learning methods are automatic and adapt to the data by learning, and as a result provide a general adaptable framework for seizure detection. These algorithms have three different stages: feature extraction, data training, and classification analysis. Artificial Neural Network (ANN) and Support Vector Machines (SVM) are the most commonly used algorithms for seizure detection problems. Many of the implemented system's performances

are discussed and compared in Tzallas et al. [28] and Orosco et al. [17].

2.1. Artificial Neural Networks (ANN)

An artificial neural network is a mathematical description of a biological neural analogy, which uses the information that is fed into it to build a network of neurons and connections to classify the data. In the training phase features used as input to the network in order to make it self-organize and achieve the desire input-output relationship [17]. Due to its high learning capability, ANNs are very useful in seizure detection task, although implementation of the system is more computationally intensive, and depending on the requirements and experimental setup might not be the best solution.

2.2. Support Vector Machines (SVM)

Support vector machines are supervised learning algorithms. During the training phase, SVM algorithm use the solution to the well known optimization problem and build an optimal high dimensional hyperplane that categorizes data into seizure and non-seizure events [17].

CHAPTER 3

MATERIALS AND METHODS

This project aims to characterize the seizure events in the rat tetanus toxin model of temporal lobe epilepsy in order to identify proper metrics for real-time automated early detection of seizures. Further efforts would make progress towards a real-time implementation of the algorithm for closed-loop optogenetic experiments studying epilepsy. The implemented system will be capable of timely identification of seizure events and delivering stimulation upon onset of these events. This chapter describes the experimental setup for recording the data, analysis methods for characterizing data, and the offline detection algorithm.

1. Experimental setup

1.1. Epilepsy model

The epilepsy model used in this study was the tetanus toxin model of the temporal lobe epilepsy. Anesthetized rats were injected with 25 ng of tetanus toxin in 0.5 µl phosphate buffered saline with 0.2% bovine serum albumin in the dura [29]. The rate of spontaneous seizures in this model are about 30 seizures per day for two weeks following the occurrence of the first seizure [30]. Seizures were defined as epileptiform events lasting more than five seconds [29].

1.2. Recording

In the experimental setup a 16-channel microelectrode array, with two rows of

electrodes capable of recording simultaneously from the hippocampal CA1 and CA3 layers, was implanted into the dorsal hippocampus. The signal that was used for the detection of the seizures is the local field potential (LFP) of the hippocampus neurons. Multi-channel LFP recordings contain information about small number of the neurons with high spatial resolution, and are a monitor of the local electrogenesis activity [31]. LFP recordings were captured using NeuroRighter (NR), an open-source hardware and software platform for stimulation and recording experiments [32]. Samples were recorded at rate of 2000 samples per second (2 kHz).

1.3. Software

Detection algorithms were implemented in MATLAB platform, and used Chronux signal processing toolbox [33] for cross correlation and spectral analysis. The custom software is capable of identifying seizure events in a LFP recording input and providing time points for the onset and offset of these events.

2. Data analysis

Data analyses of the recorded voltage traces were performed for identifying potential metrics to distinguish seizure events.

2.1. Spectrographic analysis

Spectrographic analysis was performed utilizing Fast Fourier Transform (FFT) in order to break LFP signals into their frequency contents. FFT was done using 10 seconds moving window with 1-second overlap, and with zero padding for a better frequency

resolution. Signal was filtered for frequency band of interest including only 0-70 Hz components. LFP signal was averaged from channels 1-8 for CA1 region and channels 9-16 for CA3 region. For calculation of spectrograms, Chronux mtspectrogramc function was used. This function is a multi-taper time-frequency spectrum calculator for continuous processes.

For coherogram calculations, LFP data from channel 1 for CA1, and LFP data from channel 9 for CA3 regions were used as the inputs for Chronux cohgramc function; this function is a multi-taper time-frequency coherence calculator. The coherencies between the two regions were calculated and mapped in a coherogram.

2.3. Cross-correlation

Cross-correlation was calculated between consecutive 1-second windows of LFP signals. Chronux xcorr function was used for estimating the correlation between the two signals. In each of these windows, maximum and average correlation values were calculated.

2.4. Line-length

Line-length values were calculated using 1-second windows of the signal. In each 1-second window, difference between the consecutive points were calculated and averaged for the total duration.

3. Offline seizure detection algorithm

Identified features were implemented in an algorithm to detect the seizure events in recorded data. The input for this program was a 30-minute long, 16 channels of recorded LFP

data. These data were divided into 3 different 10 minutes long sections that were analyzed separately. Line-length, maximum cross-correlation and mean power spectral density in 12-25 Hz were calculated for channels 1 and 9 of the recorded LFP as a representative for CA1 and CA3 regions of the hippocampus. The algorithm outputted detection of seizure event for each of the features separately by indicating starting and end time point of the seizure event.

3.1. Detection criteria

Custom thresholds were chosen for each of the three metrics. In the algorithm, seizure events were defined as parts of the signal that exhibited values above threshold for greater than 5 second. A secondary criterion for an event to be considered as a seizure was presence of the event in both CA1 and CA3 analysis.

CHAPTER 4

SEIZURE SIGNAL CHARACTERIZATION

Seizures in general are characterized by fast, excess neuronal activity in a synchronous manner. They are more synchronous oscillations in comparison to other signals from the brain. This chapter aims at electrographic investigation of the seizure events in the tetanus toxin model of the epilepsy, and extracting temporal and spatial features that could be used for distinguishing seizure events from the rest of the brain activity.

Local field potential is an electrophysiological signal recorded using depth electrodes. This signal represents the voltage produced by sum of the synaptic activity from all the nearby dendrites [31]. In case of the seizure, there is a prolonged increase in LFP amplitude as illustrated in **Figure 1**. **Figure 1 a, c** are showing the inter-ictal activity, and **Figure 1 b, d** are representing presence of a seizure event as marked by a red line. By comparing these 4 graphs, one can distinguish the seizure based on the increased amplitude. Another change that is seen in epileptic animals is the occurrences of inter-ictal spike; these spikes are short duration, large amplitude events that appear in the signal during non-seizing states. Inter-ictal spikes are marked by a red star in the **Figure 1 a, c.**.Note how these events are observed at a similar time in signals from both CA1 and CA3 regions of the hippocampus. This is due to the fact that pathologic features of the epileptic signal synchronize across the different hippocampal cell layers. As shown in **Figure 1 b, d** the seizure events also occur in timely fashion in both cell layers, demonstrating the synchronous spatial spread of these events in the brain.

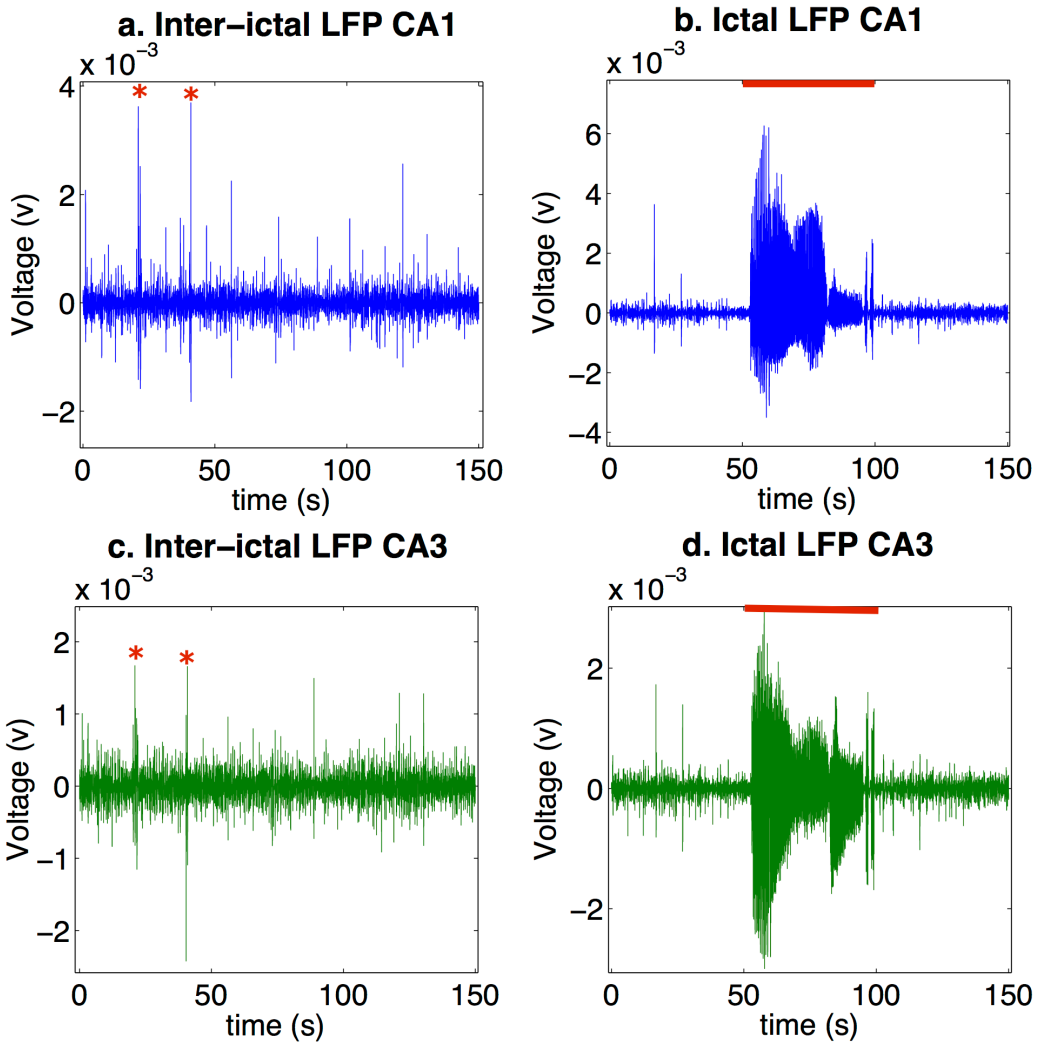

Figure 1 - Voltage trace for 150 seconds segments of the signal- (a) And (c) are representing the inter-ictal period in CA1 and CA3 regions of hippocampus respectively. Red stars in the figure mark inter-ictal spikes. (b) And (d) are representing the ictal activity with occurrence of one seizure event (marked by red line) in CA1 and CA3 regions of hippocampus respectively, note the similar timing of the events. The convention of green color for CA3 signals and blue for CA1 signals are maintained throughout this work.

In order to have a more quantitative understanding of unique characteristics of seizure events in terms of their amplitude and synchronicity, LFP signals were characterized in both time and frequency domains.

1. Frequency domain analysis

1.1. Power Spectral Density

First step in frequency domain characterization of the signal was breaking the LFP recordings into their frequency contents using a Fast Fourier Transform (FFT). FFT was done with zero padding for a better frequency resolution using 10 seconds moving window with 1-second overlap. The signal was filtered for the frequency bands of interest including only 0-70 Hz components.

The signal was initially mapped in its frequency domain by means of a power spectral density (PSD) plot as illustrated in the **Figure 2**. PSD plots are capable of showing the power associated with each frequency components of the signal. Maximum power for the signal was observed in hippocampal theta range (6-10 Hz) corresponding to awake and behaving animals. Comparison of the ictal and inter-ictal states showed a detectable increase in power associated with higher frequency bands (15-40 Hz). In the inter-ictal states in both hippocampal regions, all the power was only concentrated in 0-15 Hz, and power for frequencies above 20 Hz was zero (**Figure 2 a, c**). While in seizing state in addition to the first power peak at 7 Hz, there is a second peak in 17 Hz (**Figure 2 b, d**). Also the overall power of the signal is greater across all the frequency ranges for the seizing state.

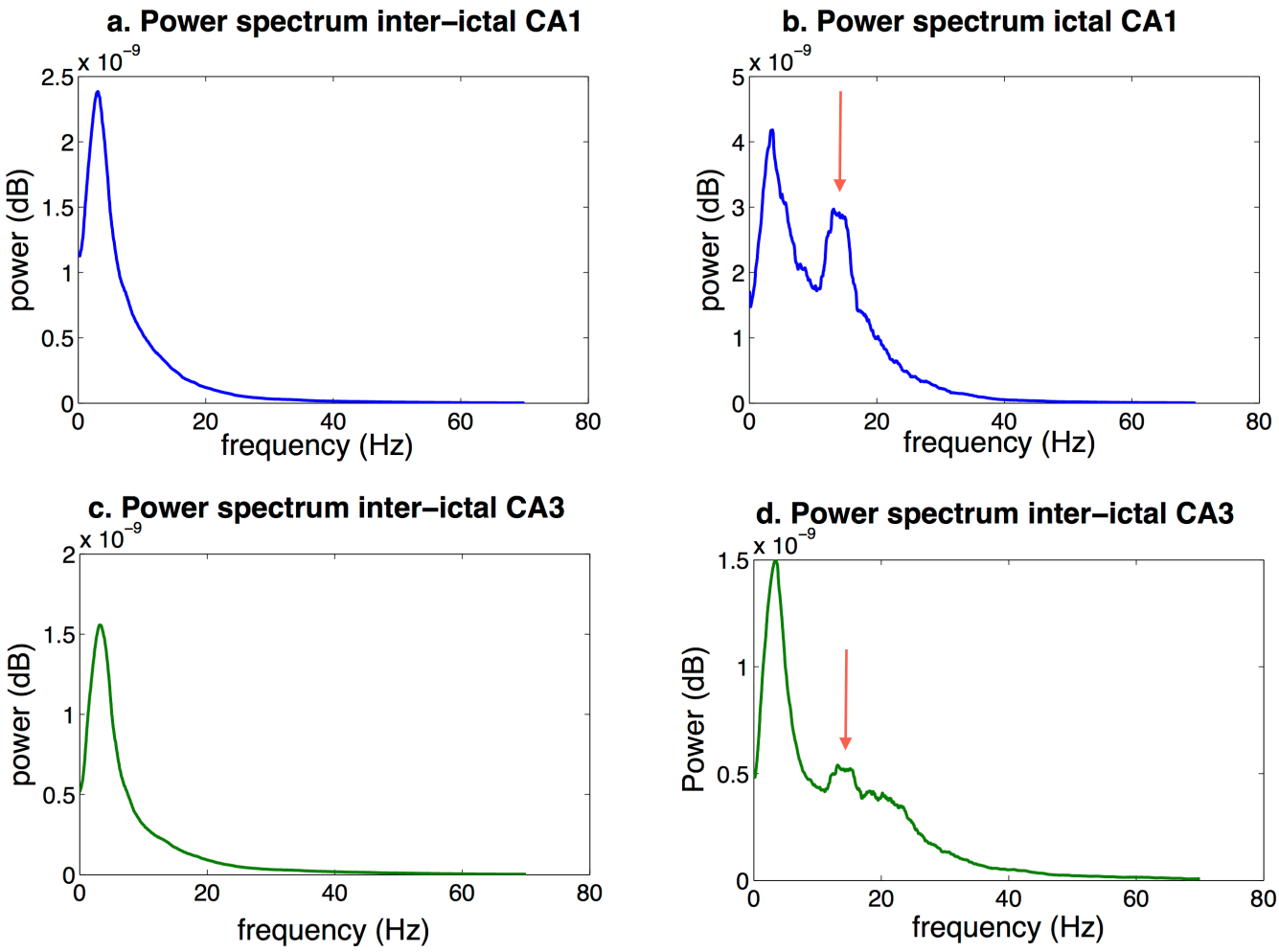

Figure 2 - Power spectral density of ictal and inter-ictal signal in CA1 and CA3 regions – As shown in the figure in case of ictal activity (c, d), in addition to increased power in the frequency components presented in the inter-ictal activity, there is an increase in power for higher frequency components of the spectrum (red arrows).

2. Time-Frequency domain analysis

2.1. Spectrogram

PSD plots have a good frequency domain resolution and provide insights on power associated with each frequency, but in order to specifically understand the changes during the seizure events, one needs to be able to link the changes in seen in frequency domain with temporal appearance of the seizure events. As a result the spectrographic analysis of the

signal was performed. Inter-ictal (**Figure 3**) and ictal (**Figure 4**) signal are illustrated in their time-frequency domain in spectrograms. These graphs clearly illustrate the increased power associated with the seizure events, as well as a similar effect during inter-ictal spikes.

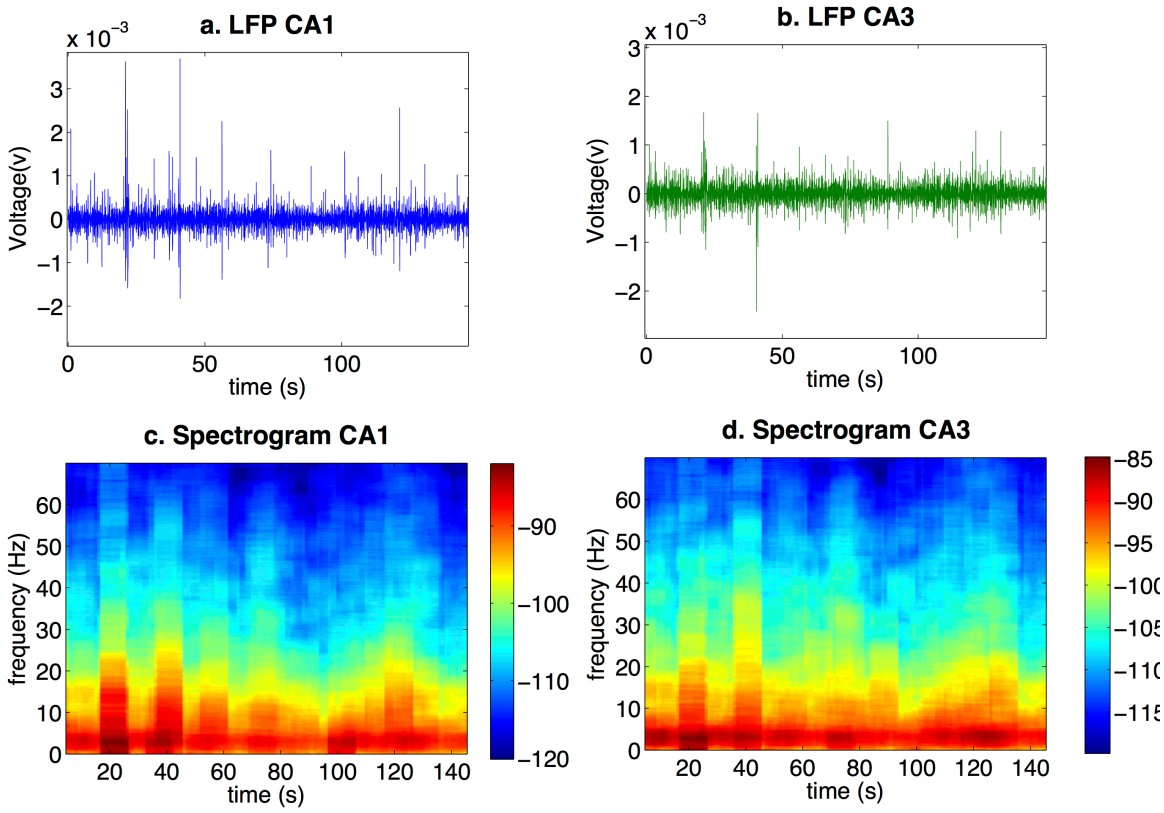

Figure 3- Inter-ictal spectrogram- Spectrogram for 150 seconds of an inter-ictal recording is shown. Parts a and b are showing the LFP in CA1 and CA3 region of hippocampus respectively. Under each LFP there is the associated spectrogram. As shown the power is concentrated in theta range (6-10 Hz) and during the inter-ictal spike events increase power is noticable.

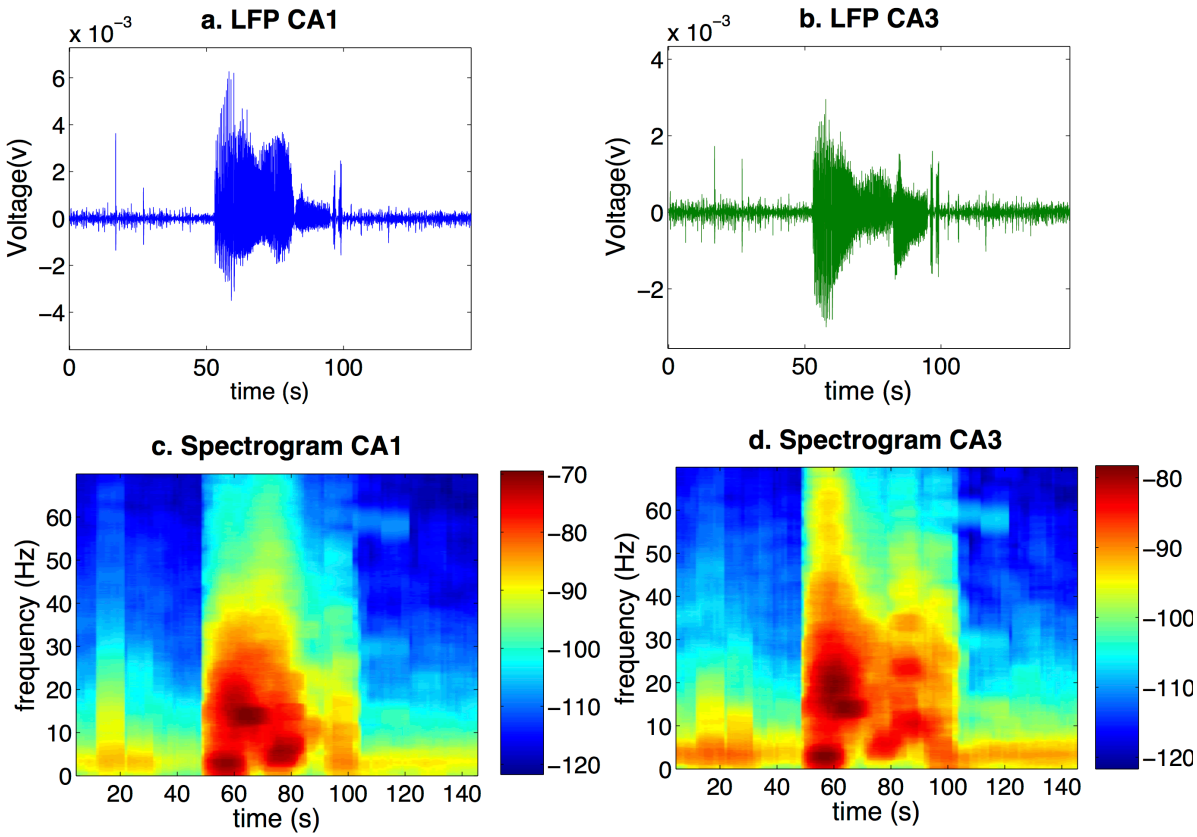

Figure 4 – Ictal spectrogram Spectrogram for 150 seconds of an ictal signal is shown. Parts a and b are LFP in CA1 and CA3 region of hippocampus respectively. Under each LFP there is the spectrogram. As shown during the seizure event there is an increase in power across all the frequency components with most of the power concentrated in 0-30 Hz frequency band.

2.2. Coherogram

The analysis done in the time and frequency domains so far only provided information about the power changes during the seizure events in relationship to time and frequency contents of the signal. Comparing data from both cell layers of the hippocampus (CA1 and CA3) indicated that these events are seen at the same time in both regions. However, a more in-depth quantitative analysis is required for understanding this relationship. Coherency is an effective measure to show the relationship between the timing of the two signals, and how often they occur together. Coherogram computes coherency

between two different signals in time-frequency domain and indicates the cross-spectral coherency. **Figure 5** calculates the coherogram between the two spectrograms for CA1 and CA3 shown in **Figure 3** and **Figure 4**. In **Figure 5** during the inter-ictal state there is high coherency in all times across many different frequencies, while in the ictal segment during the seizure event, high coherency is localized in a narrow frequency band (0-30 Hz). The narrow band localization of coherency is an indication of synchronous activity between two signals in a defined frequency. As a result the coherogram quantitatively confirms synchronicity of the activity between CA1 and CA3.

3. Time domain analysis

3.1. Cross-Correlation

As discussed at the beginning of this chapter, another feature of the seizures is the rhythmic pattern of the signal. Unlike the other periods of the LFP signal, activity during seizure is more regular. In chapter 2, cross correlation was introduced as a metric for capturing rhythmicity of the signal. This metric was calculated for comparing 1-second long consecutive windows of the LFP signal. Then in each window maximum and mean values of the cross correlation were calculated.

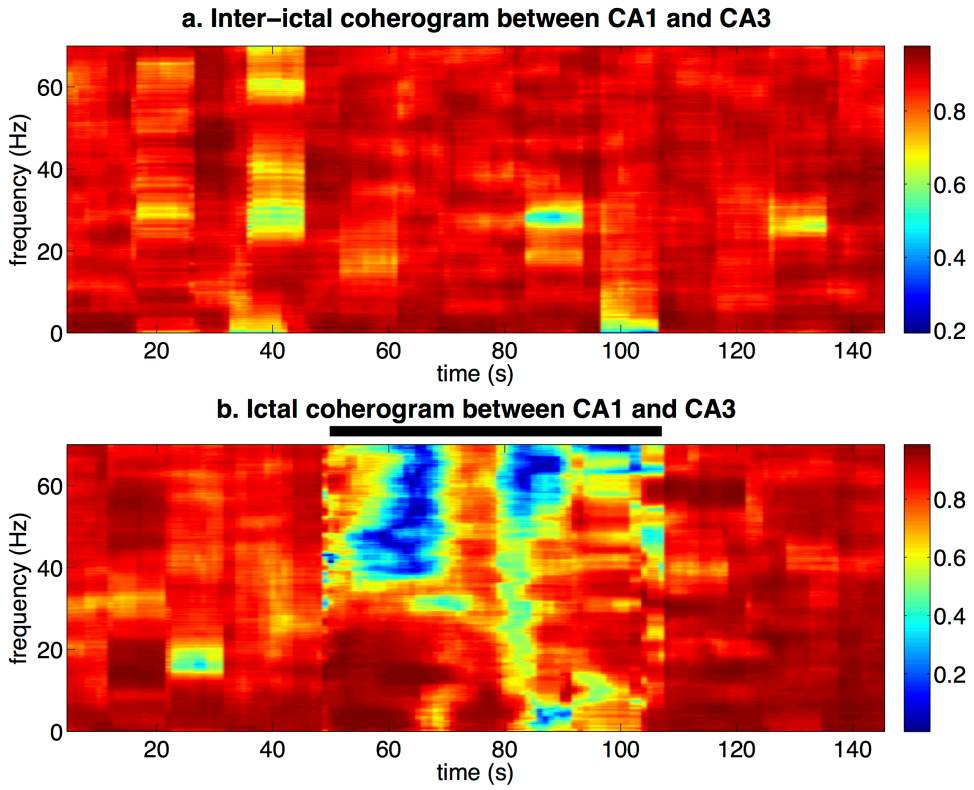

Figure 5 – Cross-spectral coherogram between CA1 and CA3 in inter-ictal and ictal states. Raw LFP recording and corresponding spectrogram of inter-ictal and ictal signals used for calculation of coherogram are shown in Figure 3 and 4 respectively. As shown in part a, in case of inter-ictal signal there is spread high coherency across all the frequency components, while in part b, during the seizure event (marked by black line) higher value of coherency (darker red) is concentrated in a narrower frequency band (0-30 Hz), indicating coherency between CA1 and CA3 regions spectrogram.

Figures 6 and 7 are illustrating the difference between the non-seizing and the seizing states for this measure. As indicated by these figures during the seizure event there is an increased cross-correlation corresponding to a less random signal. Value of the maximum cross-correlation is higher and more distinguishable during the ictal activity in comparison to the mean value of cross-correlation.

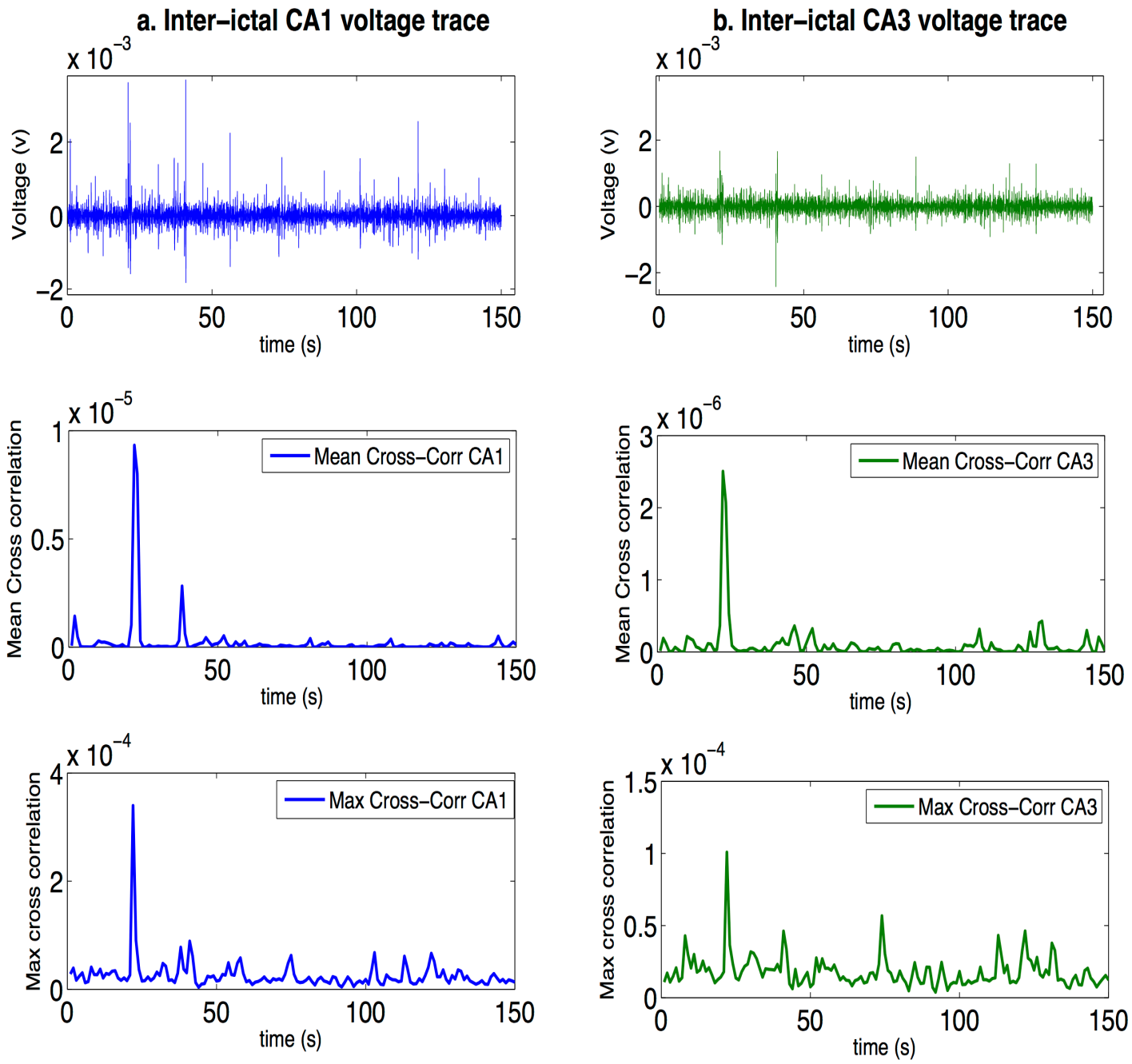

Figure 6 - Cross correlation of the inter-ictal signal – Cross correlation for a 1 second sliding window is calculated for the signal; mean and maximum value of the cross-correlation is calculated for each window. There is an increase in maximum cross-correlation during inter-ictal spikes. Part a shows the values corresponding to CA1 region and part b shows them for CA3 region. As shown similar activity is observed at similar timing in both regions.

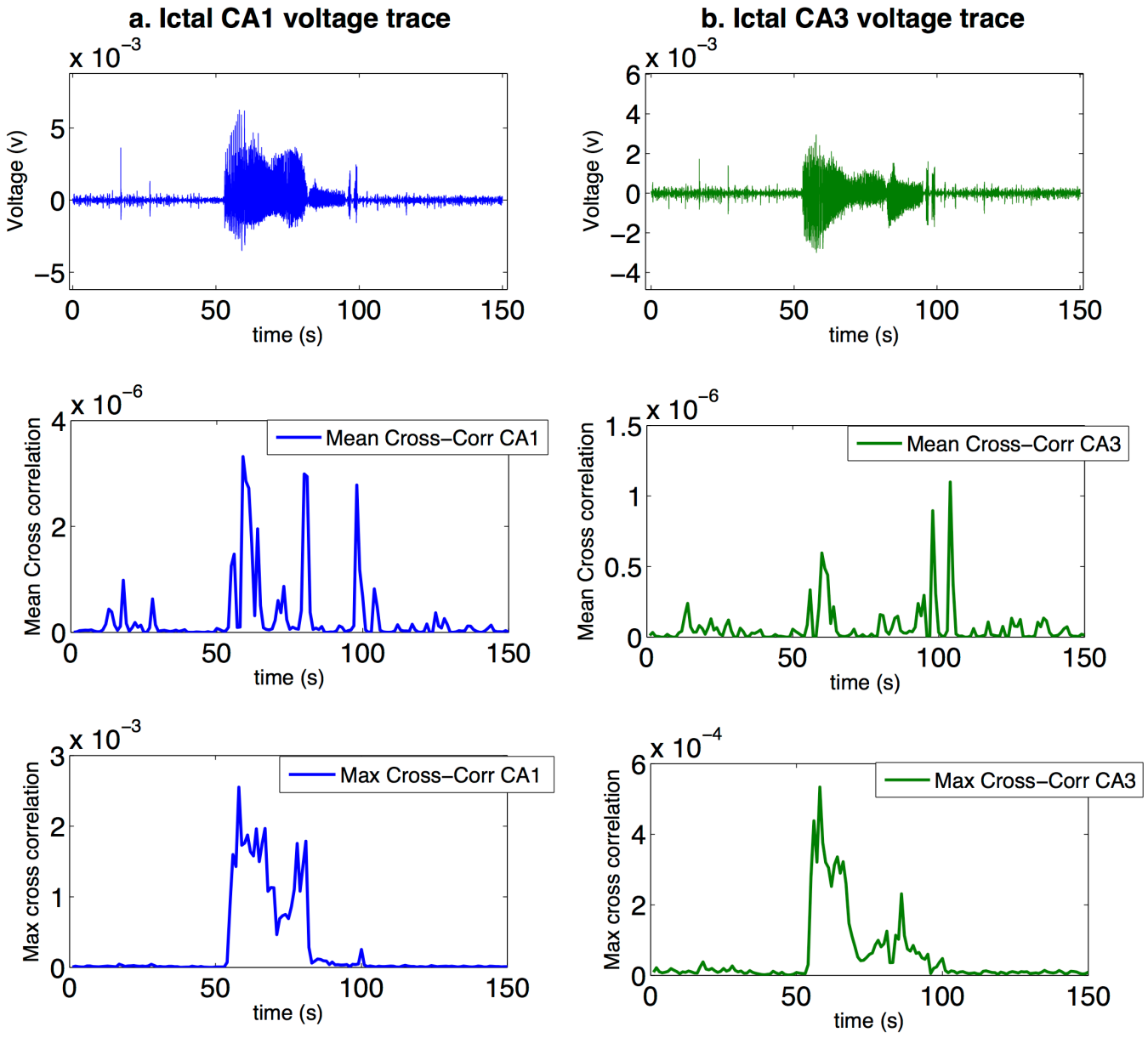

Figure 7 - Cross correlation of the seizure signal – Cross correlation for the 1 second sliding window is calculated for the signal; mean and maximum value of the cross-correlation is calculated for each window. The value of maximum cross correlation increases abruptly during the seizure event. Part a shows the values corresponding to CA1 region and part b shows them for CA3 region. As shown similar activity is observed at similar timing for both measures.

3.2. Line-Length (LLN)

Another time domain analysis that was used to characterize the seizure events was line-length (LLN). In chapter 2 LLN was introduced as a measure capable of capturing rate

of change of the data by measuring the difference between the consecutive points. Since in the seizure state neurons are firing faster [34], rate of change of the signal is expected to be higher. LLN value was calculated for the LFP recording in a 1 second time windows by averaging the difference between the consecutive points of data in each window. **Figure 8** illustrates how the fast activity is demonstrated by the LLN; as shown during both inter-ictal spikes as well as seizure events LLN value is an order of magnitude higher in seizing states than in non-seizing states.

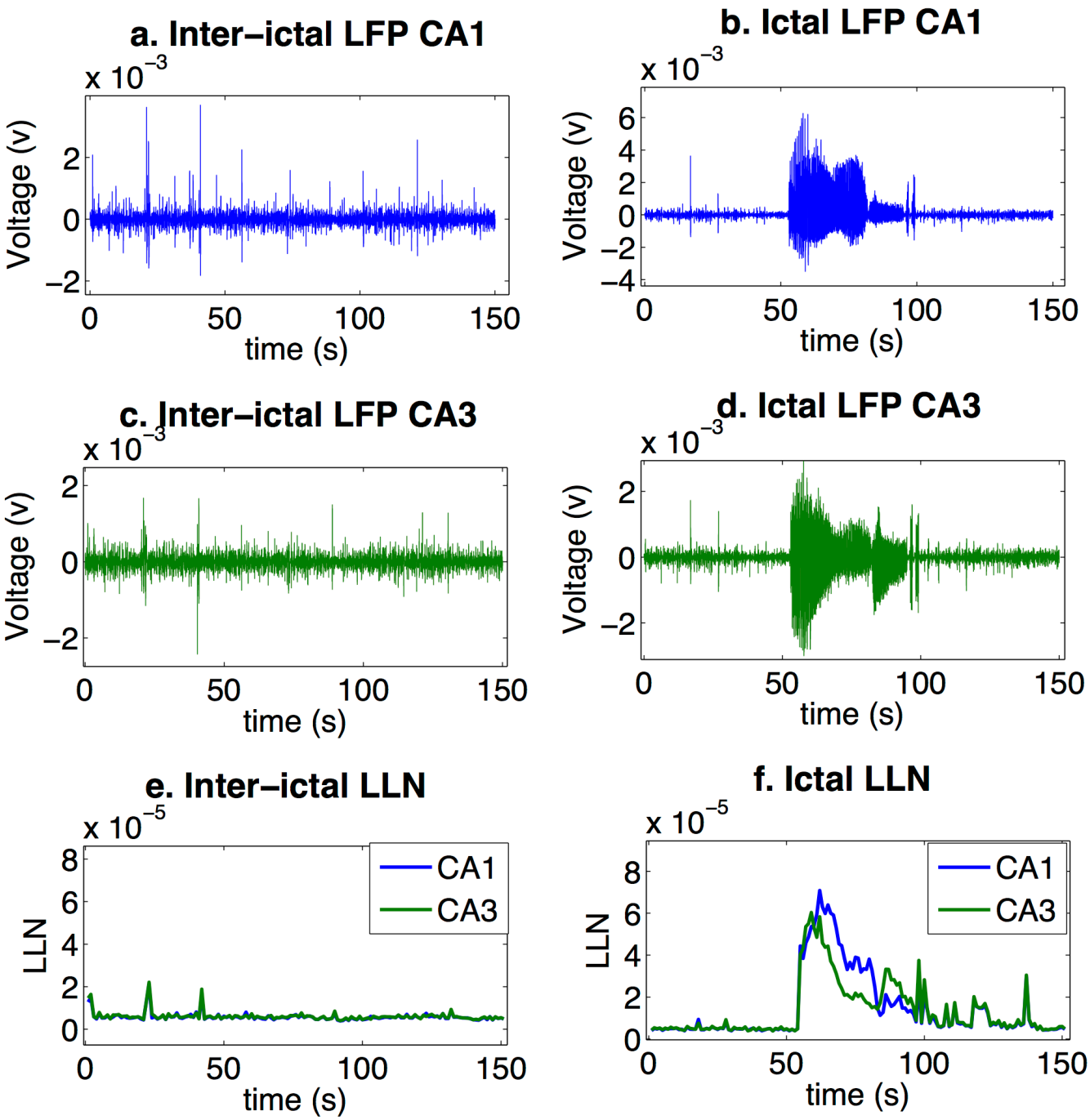

Figure 8 - Line-length analysis – LFP values for in case of inter-ictal and ictal activity are shown for both CA1 (a, b) and CA3 (c, d) regions. Corresponding line-length value is calculated in 1-second windows of the signal for both inter-ictal (e) and ictal (f) cases; there is a prolonged increase in this value during the seizure events, and a smaller increase during the inter-ictal spikes. The value for both CA1 and CA3 regions are similar and increased at the same time.

Summary of seizure events characteristics

In this chapter time, frequency and time-frequency domain metrics were used in order to characterize the seizure signals in attempt to identify potential markers for detecting seizures. Frequency and time-frequency domain analysis, using PSD and spectrograms, showed clear increases in the power of higher frequency (15-25 Hz) content of the signal associated with the seizure events. Moreover we used a coherogram to evaluate the coherency between CA1 and CA3 regions of the hippocampus in ictal and inter-ictal periods, and determining that spectrographic changes are appearing synchronously in the two regions during seizure events. Furthermore, results of time domain analysis using cross correlation and line length demonstrates that changes in these measures can be correlated with the onset of seizure events.

CHAPTER 5

OFFLINE ANALYSIS

In the previous chapter, electrographic analysis of the recorded data helped with identifying several effective measures for isolating seizure events. In order to assess the efficacy of these measures in identifying the seizure events, they were implemented in a MATLAB program for offline analysis of 480 minutes of recorded LFP. Visual examination of this data indicated the presence of 27 seizure events, as well as numerous inter-ictal spikes.

Metrics

In accordance with the initial characterization of the seizure signal, mean power spectral density (MPSD) in the 12-25 Hz frequency band, maximum cross correlation (MCC), as well as line length (LLN) were chosen as metrics in the algorithm to distinguish the seizure and non-seizure events. These metrics were independently applied on the data. In order to have a close resemblance of the real-time situation, analysis was done in 1 second sliding windows. Most of these metrics were unable to distinguish seizure events from inter-ictal spikes; consequently a duration of >5 seconds was implemented as an additional criterion to distinguish these two.

Moreover since the seizure events are synchronously occurring throughout the hippocampus, presence of the event in both cell layers of CA1 and CA3 of hippocampus was considered as another criteria for identification of seizure events. However, in order to minimize the computational cost, rather than all 16 channels, only channel 1 and channel 9 –

as representative recordings from CA1 and CA3 regions of hippocampus – were used for seizure detection.

Performance Assessment

Performance of the algorithm was assessed for sensitivity, specificity and detection latency. Detection latency was determined by calculating difference between start time by visual inspection and the algorithms determination of the start time point. Sensitivity and specificity were calculated based on the following formulas:

$$\text{Sensitivity} = \frac{True\ Positive}{True\ Positive + False\ Negative} \times 100$$

$$\text{Specificity} = \frac{True\ Negative}{True\ Negative + False\ Positive} \times 100$$

In the ultimate experimental setup the goal is to capture all the seizure events and deliver stimulation shortly after onset of every seizure. As a result, a sensitive algorithm with low detection latency was favored. Lower values of specificity corresponding to a high rate of false positives, but these were considered acceptable.

Line-Length

As discussed earlier LLN serves as a measure for capturing the rate of change in the voltage data. With adjusted threshold, this measure is capable of effectively identifying seizure events (**Figure 9**) and has perfect sensitivity (100%) and low detection latency (0.76 ± 0.52 s).

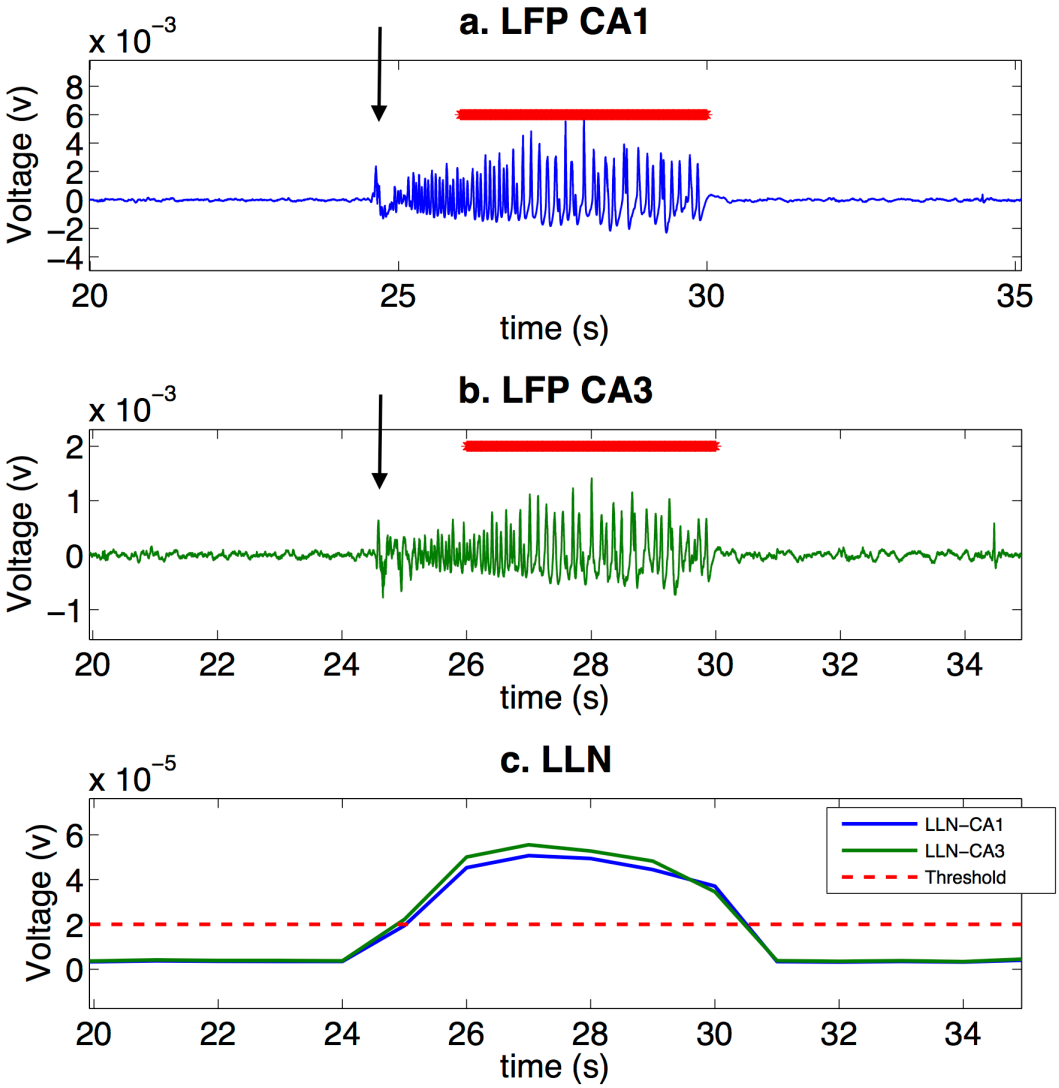

Figure 9 - LLN detection performance. LLN is capable of identifying seizure event with perfect sensitivity (100%), and relatively low detection latency. In this figure, black arrow shows visual inspection for determining event start (84.6 s) and the red line shows duration that event is identified by the LLN measure (starting at 85.7, 1.1 s detection latency). This is illustration of the LLN performance in determining beginning and end of seizure event.

However the major deficiency of this measure is high rate of false positives that is caused by fast changing data during inter-ictal spikes. This similarity causes consecutive inter-ictal spikes to be considered as a seizure event by the algorithm (**Figure 10**). But using spatial information from both CA1 and CA3 of hippocampus helped with decreasing the rate

of false positives, and increased specificity from 8.7% to 16.7%.

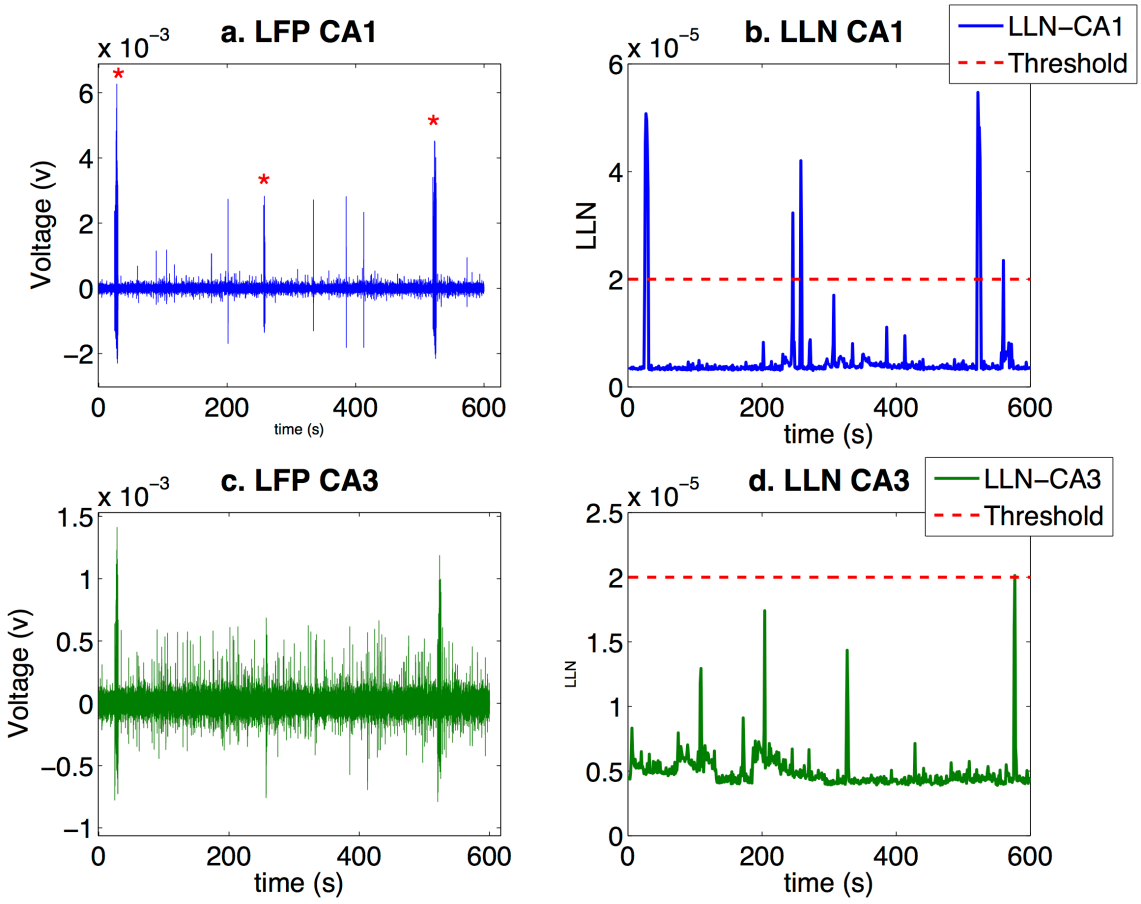

Figure 10 - False positive reduction with inclusion of spatial information for LLN. Events indicated with red stars, were previously considered as seizure events by line-length metric; however including spatial information from both CA1 and CA3 regions of the hippocampus decreased the incident of these false positives. Parts a and c are showing the recorded LFP from these two regions, parts b and d shows calculated LLN for these two regions; note the amplitude difference of LLN between CA1 and CA3.

Maximum Cross-Correlation

MCC was used as an indicator of regularity of the recorded data, that means how similar are different periods of the signal to itself. This measure was calculated based on 1 second sliding window comparison of cross-correlation value of data with itself by a 1 second lag. As discussed before, seizure events are highly regular, and as shown in **Figure 5**,

this value increases during the seizure events. Thus, MCC was used for distinguishing seizure events. Even though this metric showed high specificity (90-100%), but it is considered as an ineffective measure due to high detection latency and low sensitivity. Delays in detection were caused by high computational cost associated with calculations of this measure. The low sensitivity of the algorithm comes from the non-uniformity of this measure during different events. As an example, as shown in **Figure 12**, the algorithm is not able to pick up a seizure event due to low values of MCC in the CA3 region. These deficiencies suggest that MCC could not be use as a universal indicator of seizure events in this experimental setup.

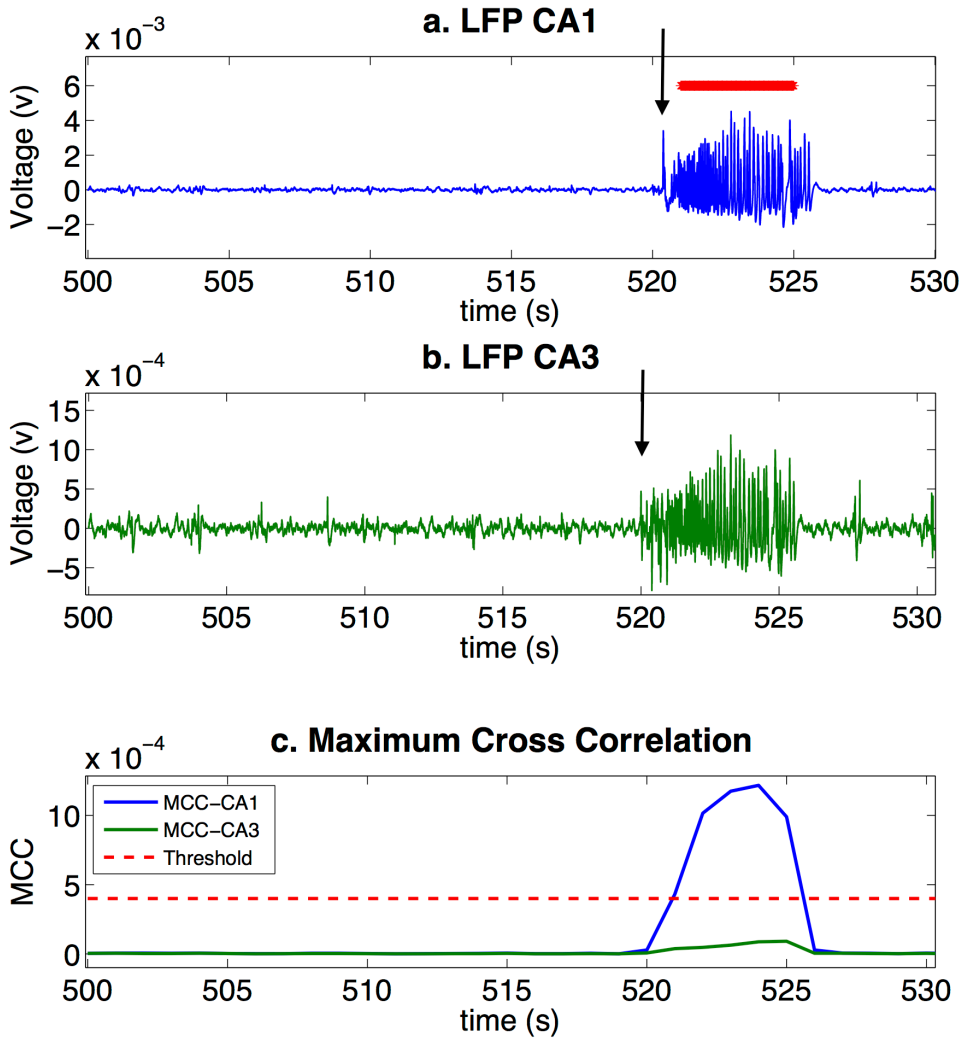

Figure 11 – MCC inability to identify seizure events. MCC values for the two different regions of the hippocampus (CA1 and CA3) are not the same, and value corresponding to CA3 region does not cross thet threshold resulting in undetected event. Sezizure event is marked by red line in the voltage trace in CA1 and is not detected by the CA3 measure. Black arrow represents start of the seizure event with visual inspection.

Mean Power-Spectral Density

MPSD was calculated by averaging power associated with 12-25 Hz frequency band in 1 second sliding window analysis of data. As shown in **Figure 2**, there is increased power in higher frequency components (15-40 Hz) of the LFP signal during seizure events. MPSD was effectively capable of capturing seizures with high specificity (96.43%) and low

detection latency of less than a second (0.24 ± 0.17 s). Moreover unlike LLN, MPSD has a relatively high specificity of 70%. As you can see in the **Figure 12**, during the seizure, MPSD value is higher than threshold in both CA1 and CA3 regions of the hippocampus. Threshold for this measure is set really low due to the fact that when there is no seizure, MPSD value is close to 0.

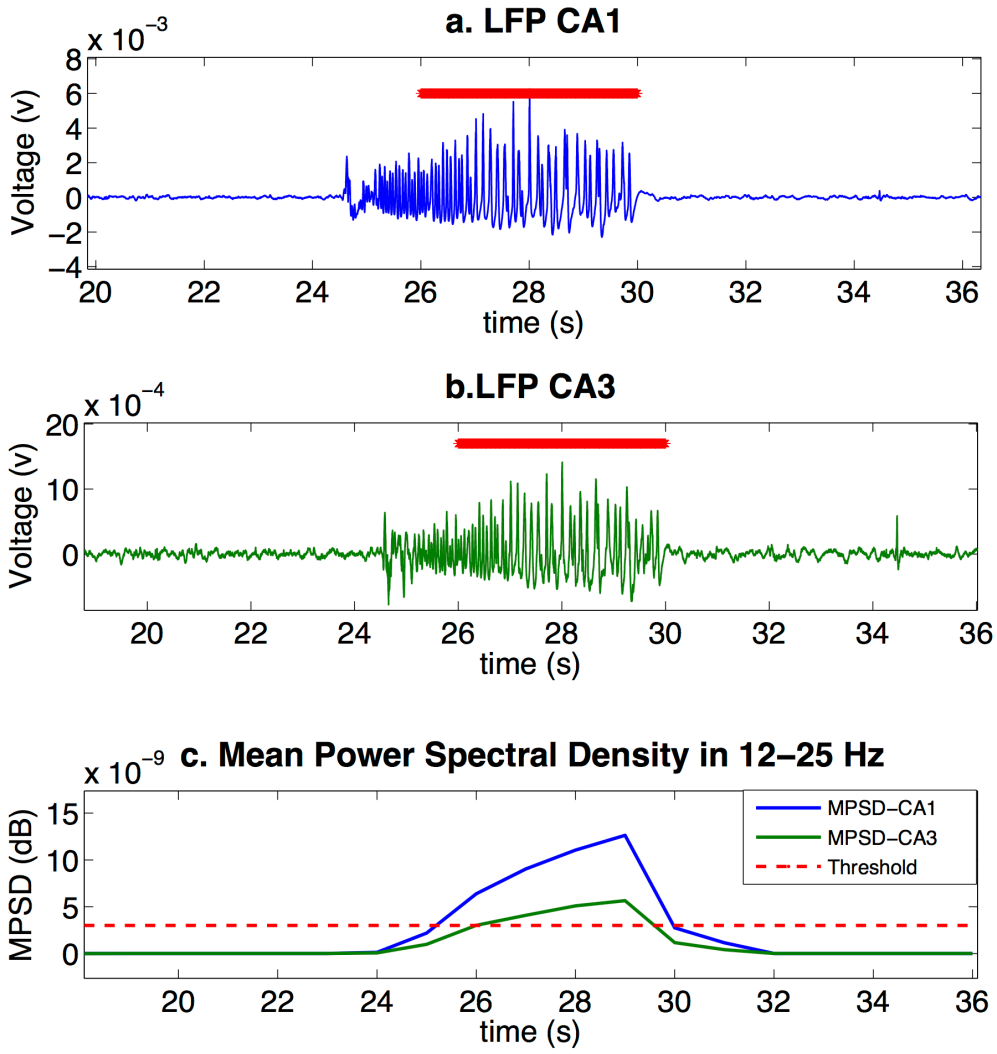

Figure 12 - MPSD identifying the seizure. MPSD is capable of effectively identifying seizure events early during the onset (0.85 s). Black arrow corresponds to visual detection of seizure onset and red line corresponds to the event as defined by the algorithm. As it is illustrated in the figure, since the threshold is really low for MPSD, although mean power in the CA3 region is lower than CA1 region, it is still effectively capable of identifying the event using the spatial information.

Comparison of the detection features

Each algorithms detected seizure events depending on a pre-defined threshold. The choice of threshold was a crucial factor in detection performance. Two different choice of threshold for LLN and MCC, and one threshold value for MPSD and algorithm performance are described in **Table 1**. As illustrated in this table, decreasing the value of the threshold was accompanied with smaller detection latency and enhanced sensitivity. Increased specificity of the algorithm in the second choice of the threshold was due to inclusion of spatial information in determining the seizure events.

	LLN		MCC		MPSD
Threshold	3 E-05	2 E-05	5 E-03	4 E-04	0.2 E-08
Sensitivity (%)	54.55	100.00	60.87	67.86	96.43
Specificity (%)	8.70	16.67	90.00	100.00	70.00
Latency (s)	1.05 ± 0.24	0.76 ± 0.52	1.28 ± 0.71	0.92 ± 0.84	0.24 ± 0.17

Table 1 – Offline performance analysis of different detection features – Performance of each feature line-length (LLN), Maximum Cross Correlation (MCC) and maximum power spectral density in 12-25 Hz (MPSD) are shown in this table. For LLN and MCC two different choices of threshold are compared.

Between these three features MCC shows the least efficacious results, with lower value of sensitivity (67.86%) and higher detection latency (0.92 ± 0.84). Comparing the three features' performance illustrate that MPSD has lowest detection latency, with high sensitivity and acceptable specificity. Performance of the LLN is similar to the MPSD with exception of lower specificity. **Figure 13** represents the difference between MPSD and LLN in terms of detecting inter-ictal spikes as potential events. Not detecting the inter-ictal spikes is what makes MPSD a powerful metric for recognizing seizure events.

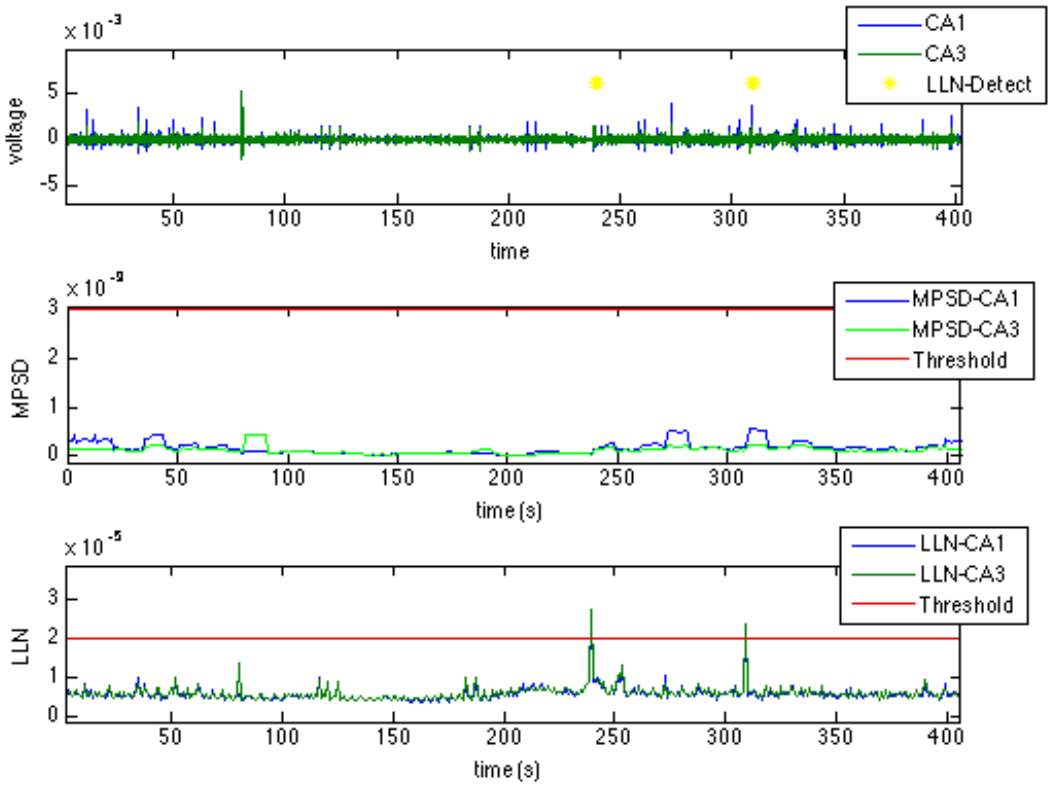

Figure 13 - **Comparison of LLN and MPSD in distinguishing the inter-ictal spikes**. As illustrated in the figure, in case of inter-ictal spikes, MPSD values are significantly lower than threshold resulting in exclusion of the spikes from seizure events. However in case of LLN, this is not true and two of these spikes that are longer are identified as seizure events.

CHAPTER 6

DISSCUSSION AND CONCLUSIONS

The goal of this thesis was to identify an effective method or methods capable of distinguishing between ictal and non-ictal activity in an animal model of epilepsy. In order to reach this goal, a literature review and data analysis were performed, leading to the identification of possible features for detection. These features were then implemented in an offline setting in a custom MATLAB program for seizure detection. In the previous chapter Line-Length (LLN), Maximum Cross Correlation (MCC), and Maximum Power Spectral Density (MPSD) were introduced as the selected features, and used independently in the detection algorithm to evaluate their performance.

The implemented program analyzed the input signal in a sliding window, and by comparing calculated values to the threshold, as well as considering duration and spatial information from both CA1 and CA3 regions of hippocampus, it identified the presence of a seizure event.

The goal of the real-time algorithm is to be capable of identifying the seizure events early in their onset and deliver stimulation. Hence the desired algorithm for our experimental setup needs to have a high sensitivity (above 90%) and low detection latency. This would give the experimenter the desired controlled delivery of the stimulation that helps with tying the stimulation with onset of the seizures without otherwise affecting the brain. High specificity is desired, but is of lower importance, because it is more important to capture all seizure events than to not have any false positives. This is because of the fact that numbers of

the seizures are limited so the experimenter desires to arrest all of these events. Further the stimulation is supposed to not have a significant effect when they are not chronically applied on the animal.

The first step in reaching the goal was proper choice of threshold; higher values of threshold yielded to a more specific performance but this was at a cost of low sensitivity and high latency. As a result, the value of threshold was lowered and spatial information was incorporated in the analysis to enhance the execution.

Results of analyzing offline performance of LLN, MCC, and MPSD showed that with lower values of threshold LLN and MPSD are effectively capable of event identification with almost perfect performance (100% and 96.43% respectively). Lowering the threshold improved the MCC performance as well (67.86% from 60.87%), but not as much as desired.

Value of detection latency was lowest for MPSD, with a below 0.5 second latency (0.24 ± 0.17), while LLN, with mean value of 0.76 ± 0.52 s, and MCC, with mean 0.92 ± 0.84 s delays, were slower at identification of seizure events.

Lastly in terms of false alarm rates, MCC had the lowest rate of false positives with perfect specificity of 100%, while MPSD and LLN showed lower specificities. MPSD was better than LLN, with 70% specificity in comparison to 16.67% specificity for LLN. LLN identified many consecutive inter-ictal spikes as seizure events, while this was not the case for MPSD (see **Figure 13**).

These results illustrate that MCC is not a suitable feature for seizure detection in this experimental setup due to high latency, low spatial resolution, and low sensitivity. Further both MPSD and LLN are identified as proper features in the early determination of ictal activity, and could potentially be implemented in real-time algorithms. They both have low

detection latency, high sensitivity, and meet the desired criteria for experimental setup.

The next goal of this study is aimed at implement LLN and MPSD as effective seizure detection features as part of a real-time seizure detection algorithm to be used in closed-loop experiments.

CHAPTER 7

FUTURE DIRECTIONS

Developing a powerful method with low computational power that is capable of early seizure detection is a subject of interest in epilepsy research. Such algorithms would make implementation of closed-loop setups possible both for clinical and research applications. This study established line-length and mean power spectral density in 12-25 Hz band as powerful features, that are capable of detecting seizure events early in their onset in the tetanus toxin model of rat epilepsy. Performance of the system is in line with desired output for a real-time setup.

In this study, choice of threshold was based on visual inspection of the signal and calculated parameters. Although this approach provided a desired output, in order to achieve the optimum choice of threshold a more systematic approach is required. Using automated assessment algorithms one could test a range of logical thresholds for each feature. Results of this analysis could be visualized by means of receiver operating characteristic (ROC) graphs for sensitivity, specificity and detection latency. Comparing the three plots together, one could make a conclusive statement about choice of the optimum threshold resulting in the optimum performance.

Optimum choice of threshold is a crucial factor in order to move toward the real-time implementation, because several features that were used in the offline analysis are unavailable in the online setting. As an example, in the offline analysis presented in this work, one of the criteria for considering an event as seizure was having greater than 5 seconds duration; in the online setting for delivering the stimulation at onset of the seizure

this information is not accessible. Moreover, having lowest value of the detection latency is another crucial factor which is going to be changed in the online setting; in a real-time algorithm the latency would be greater because of the delay caused from receiving the data as well as computational delay caused by the MATLAB wrapper.

Currently the MATLAB code based on a threshold method for seizure detection using LLN and MPSD as detection parameters is ready to be compiled and implement in C#. However, time limitations prevented real-time implementation and assessment of the algorithm. Further studies could continue the project by starting with the real-time implementation of the algorithm and testing the online performance.

References

1. *Center for Disease Control (CDC) Epilepsy fast facts*. 2013 [cited 2014 March, 5]; Available from: http://www.cdc.gov/epilepsy/basics/fast_facts.htm.

2. Wu, C. and A.D. Sharan, *Neurostimulation for the treatment of epilepsy: a review of current surgical interventions.* Neuromodulation, 2013. **16**(1): p. 10-24; discussion 24.

3. Lyons, M.K., *Deep brain stimulation: current and future clinical applications.* Mayo Clin Proc, 2011. **86**(7): p. 662-72.

4. Colom, L.V., et al., *Septo-hippocampal networks in chronically epileptic rats: potential antiepileptic effects of theta rhythm generation.* J Neurophysiol, 2006. **95**(6): p. 3645-53.

5. Gigante, P.R. and R.R. Goodman, *Alternative surgical approaches in epilepsy.* Curr Neurol Neurosci Rep, 2011. **11**(4): p. 404-8.

6. Tye, K.M. and K. Deisseroth, *Optogenetic investigation of neural circuits underlying brain disease in animal models.* Nat Rev Neurosci, 2012. **13**(4): p. 251-66.

7. Newman, J.P., et al., *Closed-Loop, Multichannel Experimentation Using the Open-Source NeuroRighter Electrophysiology Platform.* Front Neural Circuits, 2012. **6**: p. 98.

8. Fisher, R.S., et al., *Epileptic seizures and epilepsy: definitions proposed by the International League Against Epilepsy (ILAE) and the International Bureau for Epilepsy (IBE).* Epilepsia, 2005. **46**(4): p. 470-472.

9. Ivan Osorio, M.G.F., Steven B. Wilkinson, *Real-Time Automated Detection and Quantitative Analysis of Seizures and Short-Term Prediction of Clinical Onset.* Epilepsia, 1998. **39**(6): p. 615-627.

10. Frei, M., *Seizure detection.* Scholarpedia, 2013. **8**.

11. Morrell, M., *Brain stimulation for epilepsy: can scheduled or responsive neurostimulation stop seizures?* Current Opinion in Neurology, 2006. **19**(2): p. 164-168.

12. Krook-Magnuson, E., et al., *On-demand optogenetic control of spontaneous seizures in temporal lobe epilepsy.* Nat Commun, 2013. **4**: p. 1376.

13. Heck, C.N., et al., *Two-year seizure reduction in adults with medically intractable partial onset epilepsy treated with responsive neurostimulation: final results of the RNS System Pivotal trial.* Epilepsia, 2014. **55**(3): p. 432-41.

14. Wu, C. *Closed-loop stimulation: An investigational treatment for refractory epilepsy*. 2012 [cited 2014 July 22]; Available from: http://www.neuromodulation.com/fact_sheet_epilepsy.

15. Shane M. Hass, M.G.F., Ivan Osorio, *Strategies for Adapting Automated Seizure Detection Algorithms.* Medical Engineering & Physics, 2007. **29**(8): p. 895-909.

16. Jouny, C.C., P.J. Franaszczuk, and G.K. Bergey, *Improving early seizure detection.* Epilepsy Behav, 2011. **22 Suppl 1**: p. S44-8.

17. Orosco, L., Journal of Medical and Biological Engineering, 2013. **33**(6): p. 526.

18. Gotman, J., *Automatic detection of seizures and spikes.* Journal of Clinical Neurophysiology, 1999. **16**(2): p. 130-140.

19. White, A.M., et al., *Efficient unsupervised algorithms for the detection of seizures in continuous EEG recordings from rats after brain injury.* J Neurosci Methods, 2006. **152**(1-2): p. 255-66.

20. Armstrong, C., et al., *Closed-loop optogenetic intervention in mice.* Nat Protoc, 2013. **8**(8): p. 1475-93.

21. Khan, Y.U. and J. Gotman, *Wavelet based automatic seizure detection in intracerebral electroencephalogram.* Clinical Neurophysiology, 2003. **114**(5): p. 898-908.

22. Paivinen, N., et al., *Epileptic seizure detection: a nonlinear viewpoint.* Comput Methods Programs Biomed, 2005. **79**(2): p. 151-9.

23. Mormann, F., et al., *Automated detection of a preseizure state based on a decrease in synchronization in intracranial electroencephalogram recordings from epilepsy patients.* Physical Review E, 2003. **67**(2).

24. Esteller, R., et al. *Line length: an efficient feature for seizure onset detection*. in *Engineering in Medicine and Biology Society, 2001. Proceedings of the 23rd Annual International Conference of the IEEE*. 2001. IEEE.

25. Tzallas, A.T., M.G. Tsipouras, and D.I. Fotiadis, *Epileptic seizure detection in EEGs using time–frequency analysis.* Information Technology in Biomedicine, IEEE Transactions on, 2009. **13**(5): p. 703-710.

26. Bergstrom, R.A., et al., *Automated identification of multiple seizure-related and interictal epileptiform event types in the EEG of mice.* Sci Rep, 2013. **3**: p. 1483.

27. Kannathal, N., et al., *Entropies for detection of epilepsy in EEG.* Comput Methods Programs Biomed, 2005. **80**(3): p. 187-94.

28. Alexandros T. Tzallas, M.G.T., Dimitrios G. Tsalikakis, Evaggelos C. Karvounis, Loukas Astrakas, Spiros Konitsiotis and Margaret Tzaphlidou, *Epilepsy - Histological, Electroencephalographic and Psychological Aspects*. 2012: InTech.

29. Rolston, J.D., et al., *Spontaneous and evoked high-frequency oscillations in the tetanus toxin model of epilepsy.* Epilepsia, 2010. **51**(11): p. 2289-96.

30. Rolston, J.D., et al., *Electrical stimulation for epilepsy: experimental approaches.* Neurosurg Clin N Am, 2011. **22**(4): p. 425-42, v.

31. Buzsaki, G., C.A. Anastassiou, and C. Koch, *The origin of extracellular fields and currents--EEG, ECoG, LFP and spikes.* Nat Rev Neurosci, 2012. **13**(6): p. 407-20.

32. Rolston, J.D., R.E. Gross, and S.M. Potter, *A low-cost multielectrode system for data acquisition enabling real-time closed-loop processing with rapid recovery from stimulation artifacts.* Front Neuroeng, 2009. **2**: p. 12.

33. Bokil, H., et al., *Chronux: a platform for analyzing neural signals.* J Neurosci Methods, 2010. **192**(1): p. 146-51.

34. Ullah, S., *Models of epilepsy.* Scholarpedia, 2009. **4**(1409).

VITA

BAHAR RAHSEPAR

RAHSEPAR was born in Tehran, Iran. She attended middle and high school at National Organization for Exceptionally Talented (NODET) in Tehran before moving to United States of America for college. She will receive a B.S. in Biomedical Engineering from Georgia Institute of Technology in December 2014. She is planning on persuading graduate studies in Biomedical Engineering with focus on neuroengineering and computational neuroscience. Her goal is improving therapy and quality of life for patients with neural basis diseases. Besides her research and studies, she enjoys strength running, movies, and baking, as well as quality time with family and friends.